APCC
APEC CLIMATE CENTER

TECHNICAL REPORT

APCC
APEC CLIMATE CENTER

PREFACE

It is our pleasure to present to you the APEC Climate Center (APCC)'s Technical Report 2012, which reports the core outcomes of our research activities from the past year.

Since 2005, APCC, as a hub of climate information in the Asia-Pacific region, has strived to share our analysis and prediction of abnormal climate and to apply this information to regional development. The Center has established the most extensive Multi-Model Ensemble (MME) system for seasonal prediction in the world through its international science network and has provided value-added products to various stakeholders. Recently, APCC has expanded its mandate to include enhancing the capacity of APEC member economies to respond effectively to climate change and variability through better application of climate information.

In 2012, APCC continued to make an effort to improve the quality and quantity of our short-term climate forecasts and our online climate information systems, as information dissemination tools. Additionally, APCC began its endeavor to produce more applicable climate information through interdisciplinary research among various sectors, such as agriculture and hydrology. The following technical report provides more information about our research outcomes from 2012.

In 2013, following APCC's goal to enhance socioeconomic well-being through better utilization of climate information, APCC will continue to improve the quality and accuracy of its climate information, recognizing that the utility of this information is only as good as its quality. We would like to make the best use of our research outcomes in various scientific and application areas. We welcome any feedback on this report or on our services.

My best and warmest regards to all of you.

Dr. Chin-Seung Chung
Director/APEC Climate Center

CONTENTS

APCC

TECHNICAL REPORT 2012-03

An Evaluation of the Ability of CMIP5 Multi-Models to Predict Interdiurnal Variability in Present-day and Future Warming Conditions

Dr. Ok-Yeon Kim

ABSTRACT

This study assesses the performance of CMIP5 GCMs, in terms of their ability to represent mean interdiurnal variability (MIDV) of surface maximum and minimum temperatures, surface wind speed and precipitation, under present climate conditions. We assess which models exhibit the best ability to represent MIDV, and thus which models would are the most efficient in reliably projecting changes in the interdiurnal variability of a future climate. Based on the most efficient CMIP5 models chosen for each surface variable, the projected changes in MIDV in a future climate are presented. An obvious signal of marked reduction in the MIDV for surface maximum and minimum temperatures over high latitudes in cool seasons was shown; particularly in January and there was a reduction in the MIDV for surface wind speed over large land areas in the Northern Hemisphere throughout most of the year, except in January. The models also revealed a large amount of noise in the MIDV for surface wind speed. A signal of noticeable increase in the MIDV for precipitation in middle to high latitudes in the Northern Hemisphere in January was apparent, and a large increase over East Asia throughout most of the year. This study suggests a possible change in the characteristics of weather (day-to-day) in the future. These findings should be considered equally as important as findings related to mean climate change as the increasing risk of extreme weather is related to variability on daily time scales as well as to mean climate change.

1. INTRODUCTION

Climate models have historically been subjected to various tests to evaluate their performance in improving our understanding of climate variability and change. In particular, a series of phases of the Coupled Modeling Intercomparison Project (CMIP) have been designed to support climate model diagnosis, validation and intercomparison in a systematic way. Since the framework of the first phase of CMIP (CMIP1) was established in 1995, various systematic and comprehensive efforts have been made to understand and attribute climate change (e.g., IPCC 2007).

Accurate simulation of one climate facet does not necessarily mean an accurate representation of other facets, and it is therefore crucial to evaluate a broad spectrum of climate processes and phenomena in climate models (Gleckler *et al.* 2008; Pincus *et al.* 2008; Taylor 2001). Therefore, in this study we focus on the interdiurnal (day-to-day) variability as an aspect of climate because: (1) there is a good representation

of second-order moments (variability) on various time scales (e.g., interdiurnal, intraseasonal, or interannual), which is as critical as first-order moments (climatological means) in climate model assessment (Scherrer 2011); (2) there have been few studies on interdiurnal atmospheric variability in comparison with those focused on longer (e.g., intraseasonal or interannual) time scales (Kitoh and Mukano, 2009), and finally; (3) based on this research we can expect to contribute to many climate-related application sectors which intrinsically rely on an accurate representation of daily-scale variability (Prudhomme *et al*. 2002).

Before the daily output from model simulations became available, research was predominantly devoted to the investigation of the interdiurnal variability of surface temperature over a specific area using observations (e.g., Driscol *et al*. 1994; Rosenthal 1960; Williams and Parker 1997). Most of this research concentrated on the United States and the North Atlantic Ocean, where there was an accessible dataset incorporating a long period of records.

In terms of model simulations, few studies have been conducted on the importance of considering the effects of interdiurnal variability on either regional or global climate change. In addition, the majority of studies have been based only on the interdiurnal variability of surface-air temperature. A single model simulation for the present climate demonstrated that the pattern and magnitude of simulated day-to-day variability of surface temperature were generally similar to those observed. However, on doubling CO_2 levels, the model simulated a marked reduction in the day-to-day variability of surface temperature (Cao *et al*. 1992). Changes in daily surface temperature variability were also investigated by using multiple global (Kitoh and Mukano, 2009), or regional (Fischer and Schär 2009) climate model scenarios and future daily surface temperature variability was projected to increase over land in the northern Hemisphere summer and in the tropics (Kitoh and Mukano, 2009). On a regional scale, daily summer temperature variability was also projected to increase over France (Fischer and Schär 2009).

Recently, extensive daily dataset from multiple global model simulation scenarios have been made available through CMIP5 (cf. Taylor *et al*. 2012). This abundant dataset makes it possible to evaluate the daily variability for not only surface

temperature, but also many other atmospheric variables such as wind speed and precipitation. It also enables the investigation of future changes in their daily variability by using multi-model ensemble projections.

Our objective in this study was to investigate whether the future global climate would improve or deteriorate. Surface maximum and minimum temperature, surface wind speed and precipitation are sensitive variables in our lives and can affect, among other factors, the wind -chill temperature. An increase in the interdiurnal variability of the surface climate would be detrimental to our comfort, and conversely, a projected decrease in the interdiurnal variability of the surface climate; would be beneficial. To accomplish our purpose, we first examined: (1) how the observed interdiurnal variability of surface maximum and minimum temperature, surface wind speed and precipitation is represented in a reanalysis dataset, (2) how efficiently the CMIP5 multi-models resolved observed interdiurnal variability in the present climate: which models showed a greater ability to represent variability, and thus which models would be preferred for use in projecting reliable changes in interdiurnal variability in a future climate; and finally (3) the projected changes in interdiurnal variability in the future climate by the most efficient CMIP5 models. Through this study, we expected to gain knowledge of the possible features of future weather conditions under a warmer climate induced by the new developed emission scenarios of the CMIP5 projects.

2. METHODOLOGY

2.1 Reanalysis and Models

2.1.1 Reanalysis

We considered four reanalysis datasets: National Centers for Environmental Prediction (NCEP)-National Center for Atmospheric Research (NCAR) Reanalysis II (Kanamitsu *et al*. 2002; hereinafter NCEP-R2), European Center for Medium range

Weather Forecasting (ECMWF) ERA-Interim reanalysis (Dee *et al*. 2011; hereinafter ERA-Interim), National Centers for Environmental Prediction- Climate Forecast System Reanalysis (Saha *et al*. 2006; hereinafter NCEP-CFSR) and National Aeronautics and Space Administration-Modern-Era Retrospective Analysis for Research and Applications reanalysis (Rienecker *et al*. 2011; hereinafter NASA-MERRA). We also used one global precipitation dataset, the Global Precipitation Climatology Project dataset (Yin *et al*. 2004; Huffman *et al*. 2001; Bolvin *et al*. 2009; hereinafter GPCP).

Using the datasets, we focused on four daily life-sensitive surface variables; daily maximum and minimum near surface (2-meter) air temperature, daily near surface (10-meter) wind speed and daily precipitation. NCEP-R2 is the only dataset that provides daily maximum and minimum temperature: the other datasets provide only daily mean temperature. As a result, we exploited all four variables from the reanalysis datasets extending from 1979 to 2005 (27 years) and used daily precipitation from the GPCP dataset ranging from 1997 to 2005 (9 years). We selected these time-periods to coincide with the length of coverage of the CMIP5 models. Note that daily variables from four reanalysis datasets and the global precipitation dataset are interpolated onto 1.875° (longitude) by 1.875° (latitude) in order to compare the daily variables with those from multi-models.

2.1.2 Models

We used the daily output of 15 CMIP5 models, which had been prepared for participation in phase five of the Coupled Model Intercomparison Project (CMIP5) in support of the IPCC AR5. Daily outputs of the models used in this study were analyzed for three time slices: historical simulations of contemporary climate (1979 to 2005; hereinafter "hist"); one of the RCP (Representative Concentration Pathways) scenario simulations of future climate (2030 to 2056 and 2073 to 2099; hereinafter "RCP4.5 mid-21st"and "RCP4.5 late-21st", respectively). These experiments are, therefore, long-term (century time-scale) simulations, initialized from the end of freely evolving simulations of the historical period under the CMIP5 strategy (Hibbard *et al*. 2007; Meehl and Hibbard 2007). For the historical simulations, changing conditions consistent with observation were additionally imposed by including atmospheric

composition (including CO_2), solar forcing, emissions or concentrations of short-lived species and natural and anthropogenic aerosols and land use (Taylor *et al*. 2012). The RCP4.5 scenario used in this study is a stabilization scenario in which radiative forcing is stabilized at 4.5Wm-2 in 2100 and radiative forcing and CO_2 concentrations are held constant after 2100 (Clarke *et al*. 2007; Smith and Wigley 2006; Wise *et al*. 2009).

The 15 CMIP5 models evaluated in this study come from nearly all the major climate modeling groups and are detailed in Table 1. As in the case of the reanalysis datasets, we employed four daily variables including maximum and minimum near surface (2-meter) air temperature, near surface (10-meter) wind speed and precipitation from the 15 models. Since each model has a different number of ensembles for each experiment, all ensemble members for each model, experiment, and variable were first averaged. Because all models have different spatial resolutions, each variable from each model and experiment was then interpolated onto the 1.875° (latitude) by 1.875° (longitude) as performed with the reanalysis and global precipitation datasets.

Table 1 Summary of CMIP5 models used in this study

Index	Organization/ Countries	Model Identification	Atmosphere Resolution	Ocean Resolution	Number of ensembles	
					hist	rcp45
A	CSIRO, BOM / Australia	ACCESS1-0	1.875x1.25x38	1.0x1.0L50	1	1
B	BCC / China	bcc-csm1-1	T42L26	1.0x(1-1/3)L40	3	1
C	CCCma / Canada	CanESM2	T63L35	256x192L40	5	3
D	CSIRO-QCCCE / Australia	CSIRO-Mk3-6-0	T63L18	1.875x0.9375L31	10	10
E	NOAA, GFDL / USA	GFDL-ESM2G	M45L24	360x210L63	2	1
F	MOHC / UK	HadGEM2-CC	N96L60	(1.0-0.3)x1.0L40	1	1
G	MOHC / UK	HadGEM2-ES	N96L38	(1.0-0.3)x1.0L40	1	1
H	INM / Russia	INM-CM4	2.0x1.5x21	1.0x0.5x40	1	1
I	IPSL / France	IPSL-CM5A-LR	96x95x39	2x2L31	1	2
J	IPSL / France	IPSL-CM5A-MR	144x143x39	2x2L31	1	1
K	AORI, NIES, JAMSTEC / Japan	MIROC5	T85L40	256x224L5	4	3
L	AORI, NIES, JAMSTEC / Japan	MIROC-ESM	T42L80	256x192L44	3	1

Index	Organization/ Countries	Model Identification	Atmosphere Resolution	Ocean Resolution	Number of ensembles	
					hist	rcp45
M	AORI, NIES, JAMSTEC / Japan	MIROC-ESM-CHEM	T42L80	256x192L44	1	1
N	MPI-M / Germany	MPI-ESM-LR	T63L47	GR15L40	3	3
O	MRI / Japan	MRI-CGCM3	TL159L48	1x0.5L51	5	1

2.2 Analysis method

2.2.1 Definition of Mean Interdiurnal Variability (MIDV)

The interdiurnal variability (day-to-day variation) of a variable denotes the magnitude of the difference in the daily variable between two consecutive days and is abbreviated to "IDV." By averaging the IDV over the entire period for a particular month, we obtained the mean interdiurnal variability, (abbreviated to "MIDV"). The interdiurnal variability was calculated by subtracting the value of one day from that of the following day. Those daily differences were then converted to absolute values, which express the magnitude of daily change, regardless of the sign of the change. Williams and Parker (1997) stated that the absolute value of IDV captures the chronological sequence of variable change throughout a month, but the use of standard deviations or similar measures of variability, does not. Finally, by averaging the absolute value of interdiurnal variability over all the years for a particular month, we found the mean interdiurnal variability. Mathematically, the IDV and MIDV are as follows:

$$\mathrm{IDV}_{X}^{i,j}(m,y) = \Delta X^{i,j}(m,y) = \mathrm{abs}\left(X_{d+1}^{i,j}(m,y) - X_{d}^{i,j}(m,y)\right) \quad (1)$$

where X indicates each variable considered; i and j denote each grid point and m; and d and y represent month, day and year, respectively.

$$\mathrm{MIDV}_{X}^{i,j}(m) = \frac{1}{n}\sum_{y=1}^{n} \mathrm{IDV}_{X}^{i,j}(m,y) \quad (2)$$

where n means the number of years. As a result, we attained two-dimensional fields of MIDV for each variable for a particular month. The same terms and their definitions are used in literature (Driscol *et al.* 1994; Rosenthal 1960; Williams and Parker 1997).

2.2.2 Metrics for assessing MIDV

In this study, metrics are constructed to justify the models' performances in representing observed MIDV for the maximum and minimum near surface air temperature, near surface wind speed and precipitation. In developing the metrics for evaluating the MIDV from the models' simulations against those from reanalysis datasets, we computed two statistical summaries: the pattern correlation coefficient (PCC) and the root mean square error (RMSE). We also introduced a statistical measure called the variability index (VI) to analyze the performance for each model, variable and grid-point:

$$VI_X^{i,j}(m) = \left(\sqrt{\frac{MIDV_X^{i,j}(m)}{MIDV_{X,ref}^{i,j}(m)}} - \sqrt{\frac{MIDV_{X,ref}^{i,j}(m)}{MIDV_X^{i,j}(m)}} \right)^2 \quad (3)$$

where $MIDV_X^{i,j}(m)$ and $MIDV_{X,ref}^{i,j}(m)$ are the two-dimensional MIDV of the model and reference for each variable, X, for a particular month, m. Based on the definition of VI, the value of VI is always positive and unbounded above. Smaller values of VI indicate a better agreement with the reference dataset; a perfect agreement between model and reference dataset would result in 0 of VI. The basic concept of this measure is closely related to that of the quantity used by Gleckler *et al.* (2008) and Scherrer (2011), in which they used the standard deviation of the seasonal value instead of the MIDV of the daily value. The VI is a good measure in assessing the differences in MIDV between the model and the reference dataset; enabling us to identify consistent biases in the MIDV of a single model.

Using the metrics (consisting of PCC, RMSE and VI) calculated for each model, we examined how well the CMIP5 models can resolve the MIDV in the present climate. In addition, based on the metrics, we determined which models among the 15 CMIP5

models could be selected for projecting reliable changes in MIDV in the future climate.

2.2.3 Signal-to-noise (SN) ratio of MIDV

It is well known that uncertainty about how the future climate will change stems mainly from results presented by the internal variability of models, and the models' responses to increased radiative forcing and to forcing itself (Deser *et al*. 2012; IPCC 2007). These uncertainties play a significant role in determining a signal-to-noise (SN) ratio of climate change, which is considered a critical factor for climate impact studies (e.g., Santer *et al*. 2011). The SN ratio is defined as the difference between mean values in the future period (2030 to 2056 and 2073 to 2099) and those of the base period (1979 to 2005), divided by the standard deviation for the future period. It thus represents a ratio of meaningful information, or the ratio of a desirable signal to a signal noise. A ratio higher than 1 indicates a more desirable signal than noise and a ratio lower than 1 indicates a higher noise than signal. Calculating the SN ratio, we assessed how CMIP5 models are able to project the changes in MIDV in the future climate and identified how much confidence we would expect in climate change projections for MIDV. That is, the SN ratio is used here to quantify climate change uncertainty for a prescribed RCP scenario (e.g., Lobell *et al*. 2007).

3. RESULTS

3.1 Observed MIDV

We examined the observed MIDV from 1979 to 2005 calculated from each reanalysis dataset. In analyzing the MIDV for near surface daily mean temperature, we found that all reanalysis datasets exhibited a similar MIDV pattern for all months (not shown). We focused on the daily minimum and maximum temperature rather than the daily mean temperature. However, all reanalysis datasets, except NCEP-R2, included only the daily mean temperature. Hence, assuming the MIDV patterns for

daily mean temperature can reflect those for daily minimum and maximum temperature, we decided to use the NCEP-R2 dataset for daily near surface minimum and maximum temperature.

We also compared MIDV from 1979 to 2005 for near surface wind speed, computed from each reanalysis dataset. In general, NCEP-R2 presented a higher MIDV for near surface wind speed over the land and ocean, whereas other reanalysis datasets showed similar patterns and magnitude of MIDV over all areas. We therefore selected the ERA-Interim dataset for the daily near surface wind speed, in accordance with Szczypta *et al*. (2011) who found that ERA-Interim reasonably reproduced the observed near surface wind speed.

A comparison of MIDV from 1979 to 2005 for precipitation calculated from each reanalysis dataset, revealed a large inconsistency amongst the magnitude of MIDV. Because of the large difference, we also computed MIDV from 1997 to 2005 for precipitation using GPCP, as well as using all the reanalysis data. However, the magnitude of MIDV for precipitation calculated from GPCP again appeared significantly different from that computed from other reanalysis data. In this study, we decided to use the GPCP dataset for daily precipitation spanning the years from 1997 to 2005 with the purpose of comparing MIDV from the GPCP product with that from the models, even though the GPCP dataset covered a relatively shorter period than any other reanalysis data. Gebremichael *et al*. (2005) found that the GPCP daily product suitably captured the variability of precipitation and that the GPCP daily dataset was capable of detecting rainy days at a large range of thresholds. Bolvin *et al*. (2009) also concluded that the GPCP dataset adequately captured the day-to-day occurrence of precipitation and mentioned that GPCP daily fields were, to some extent, useful in meteorological and hydrological studies.

In examining the observed MIDV for each variable calculated from each dataset, we found a larger MIDV for the maximum and minimum temperature over the extratropical winter hemisphere (Fig. 1(a)-(d)). In January, the MIDV was about 3 to 4 K for maximum temperature and 5 to 6 K for minimum temperature over land in the northern hemisphere, but less than 1 K over the ocean. This was the same in July over the southern hemisphere. This result is in good agreement with that of

literature. The MIDV for temperature should be the largest in the cold season when advective temperature changes are most intense and smallest in the warm season when advective temperature changes are least intense (Rosenthal *et al*. 1960).

In addition, the MIDV for minimum temperature was larger than that of maximum temperature. In analyzing MIDV for surface wind speed (Fig. 1(e) and (f)), we found that the MIDV was the smallest over the tropics and largest over the ocean in the extratropics. In particular, the maximum value of MIDV was found over the North Pacific and North Atlantic Ocean in January. In addition, the MIDV was much stronger in the cold season than in the warm season. We also explored MIDV for precipitation (Fig. 1(g)-(h)). A larger value of MIDV for precipitation was found in the tropics, particularly along the Intertropical Convergence Zone (ITCZ). The MIDV in July was also larger in the monsoon regions including Southern Asia, Southeast Asia and East Asia, and in January it was larger around Northern Australia, South Africa and South America.

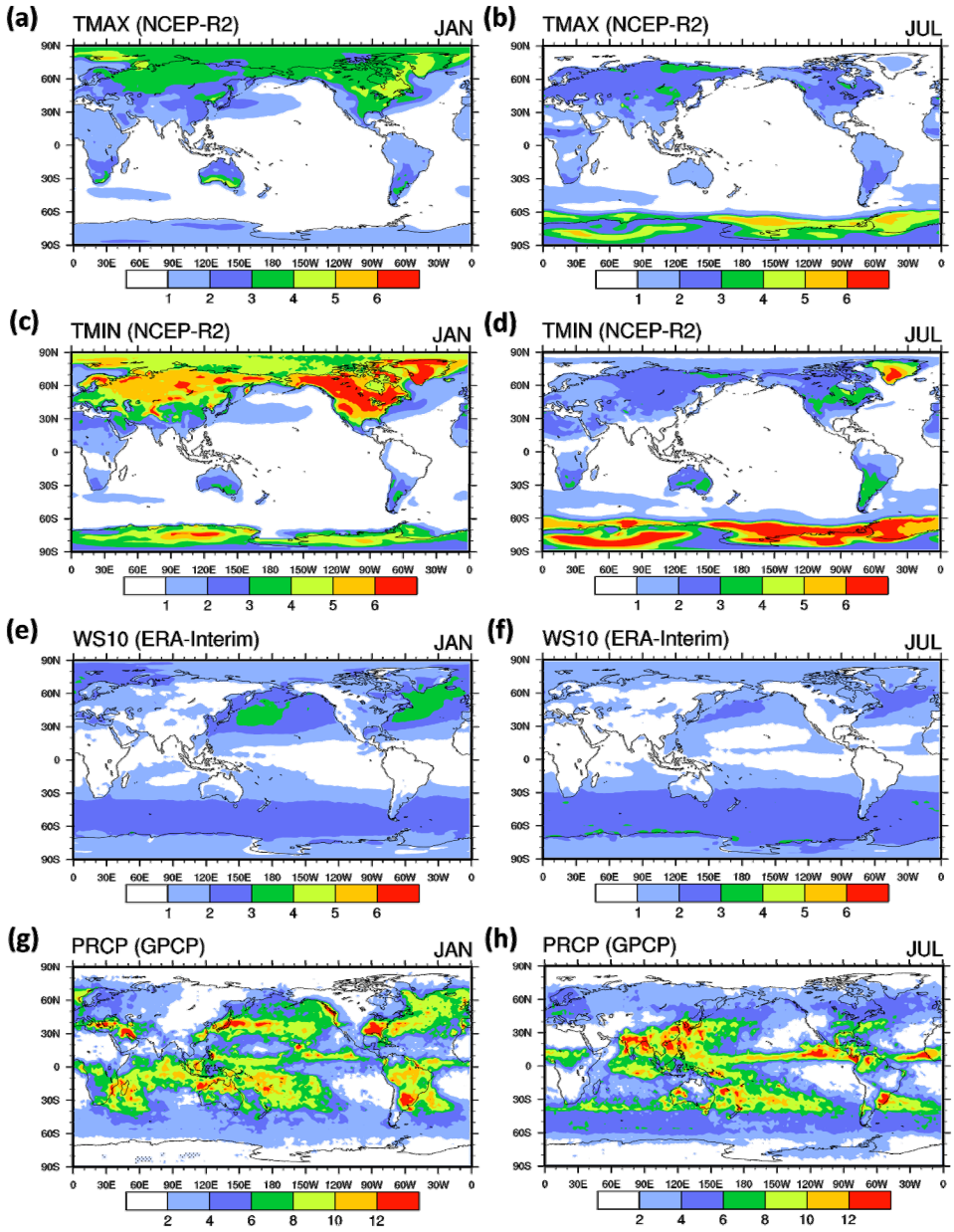

Figure 1 Observed mean interdiurnal variability (MIDV) in each reanalysis dataset and observation: (a)-(b) 2-m maximum temperature from NCEP-NCAR reanalysis 2, (c)-(d) 2-m minimum temperature from NCEP-NCAR reanalysis 2, (e)-(f) 10-m wind speed from ERA-Interim reanalysis and (g)-(h) precipitation from GPCP. Note that the dataset for daily precipitation from GPCP ranges from 1997 to 2005 (9 years), and the datasets for other variables extends from 1979 to 2005 (27 years).

3.2 Simulated MIDV: Model Evaluation

3.2.1 General features of simulated MIDV

A comparison of MIDV for near surface maximum temperature from each reanalysis dataset with that from each CMIP5 model revealed that nearly half of all models showed a similar magnitude and pattern between the simulated and observed MIDV (Fig. 2), but the remaining models exhibited a similar pattern, but weaker magnitude, than the observed MIDV. To be more specific, the models showing a similar magnitude included ACCESS1-0, GFDL-ESM2G, HadGEM2-ES, inmcm4, IPSL-CM5A-LR, and IPSL-CM5A-MR. However, the mean of all 15 multi-model (hereinafter "MMM15") MIDV showed a weaker magnitude of MIDV compared to that of the observed MIDV. Kitoh and Mukano (2009) found that the CMIP3 global model ensemble underestimated mean daily temperature variability realized in the reanalysis datasets. They also stated that this was probably related to the less developed synoptic disturbances within the models than in the reanalysis datasets. A very similar spatial feature was found in all other months and for all other variables.

From an annual cycle of land-only areal averaged MIDV for all variables (Fig. 3), we found that models' performance in representing observed MIDV over land was consistent across all months, but varied depending on the variables considered. In addition, the magnitude of observed MIDV was fairly similar to the upper bound of the magnitude of the models' MIDV for minimum and maximum temperature and wind speed (Fig. 3(a)-(c)). However, the magnitude of observed MIDV for precipitation was different from that of models' MIDV (Fig. 3(d)), which is probably because the daily variability of precipitation can be affected by isolated storms or convection, as well as different synoptic disturbances. This can make it difficult for climate models to resolve day-to-day variations in precipitation in space and time,which is to be expected as precipitation has a greater variability in space and time than the other variables, and thus climate models are expected to be less skillful at simulating precipitation (Alexander and Arblaster 2009). Nevertheless, several studies have suggested that it is still meaningful to utilize climate models when projecting the climate-change signal for precipitation in a future climate (e.g., Hagemann and Jacob

2007; Sushama *et al*. 2006). As a result, general features of the simulated MIDV (as in Fig. 2 and Fig. 3) suggest that for different variables it would be possible to select certain models which performed well in resolving observed MIDC, regardless of the month or season.

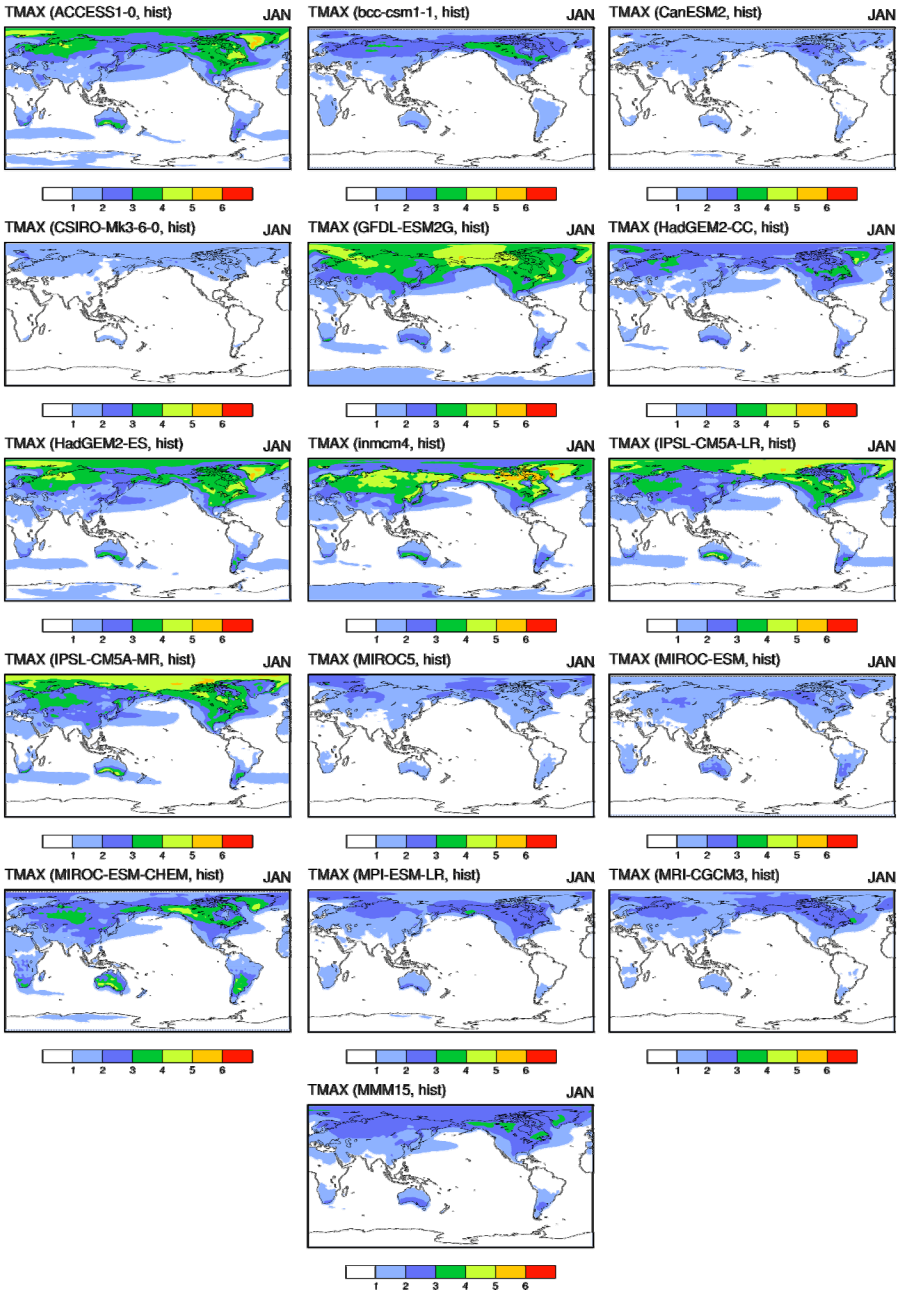

Figure 2 Simulated mean interdiurnal variability (MIDV) for near surface maximum temperature in January for 27 years from 1979 to 2005 calculated from 15 CMIP5 models and the multi-model mean (MMM15).

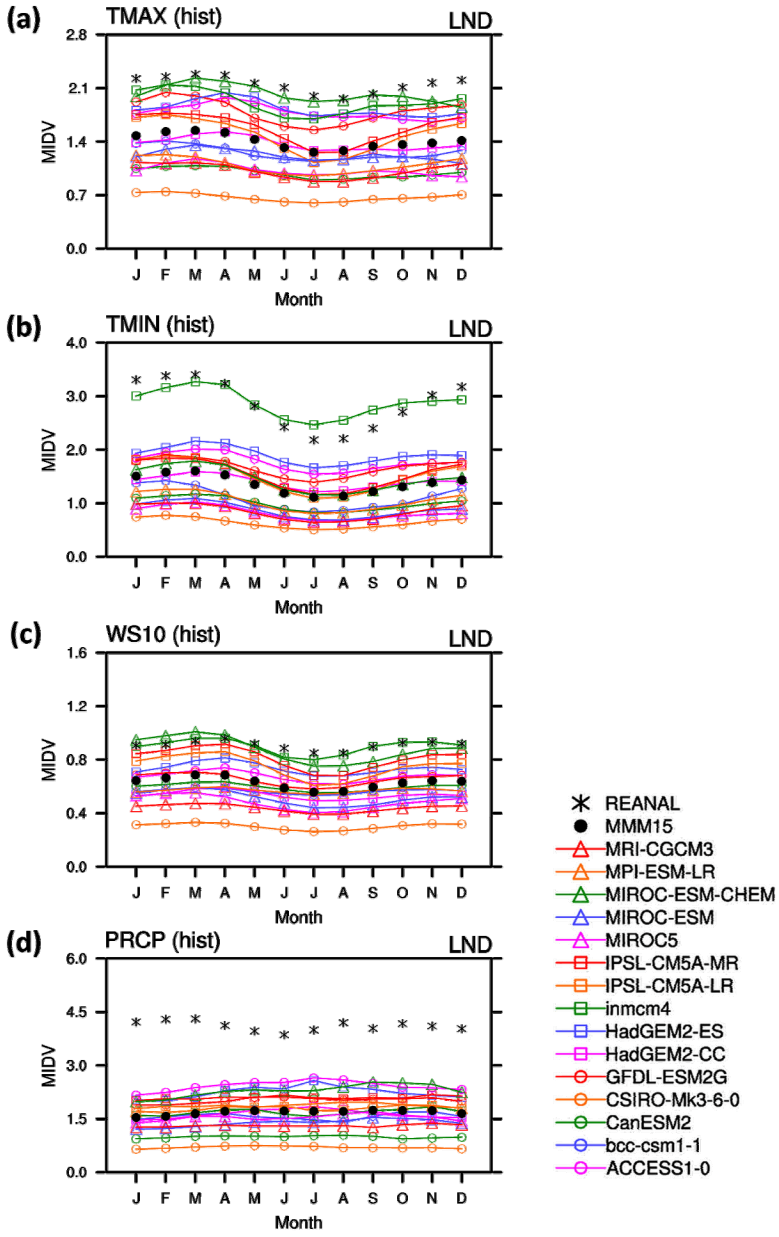

Figure 3 Annual cycle of area-averaged mean interdiurnal variability (MIDV) for (a) 2-m maximum temperature, (b) 2-m minimum temperature, (c) 10-m wind speed for 27 years from 1979 to 2005 and (d) precipitation for nine years from 1997 to 2005 calculated from reanalysis (asterisks), 15 CMIP5 models (colored lines with symbols) and multi-model mean (MMM15; black dots). Note that the MIDV over land only is considered for calculation of the area-averaged mean.

3.2.2 Selection of the best models

In consideration of the observed MIDV from reanalysis datasets as reference data, we evaluated the CMIP5 multi-models' ability to resolve the MIDV in the current climatic conditions (i.e., 1997–2005 for precipitation and 1979–2005 for other variables). In judging the models' peformance based on metrics consisting of VI, PCC and RMSE, we selected the top three best models for each variable, regardless of the month.

We first examined the spatial pattern and magnitude of the variability index (VI) as one of the metrics' factors used in this study. In analyzing the spatial pattern and magnitude of the VI for maximum temperature in July, we found that most models, with the exception of three, (bcc-csm1-1, CanESM2, and CSIRO-Mk3-6-0), exhibited a relatively small VI (Fig. 4). In addition, these three models showed a larger VI in parts of the ocean than over land, implying a lack of observation skill over the ocean: bcc-csm1-1 exhibited a large VI over almost the entire ocean and CanESM2 and CSIRO-Mk3-6-0 represented a large VI mainly over the tropical ocean. As detected in the annual cycle of MIDV for maximum temperature in Fig. 3(a), the general spatial pattern of theVI for maximum temperature was also consistent across all months. We also found that within these three models, the amount of VI shown depended on the variable considered, but for one of the variables the results were the same for all months.

We then assessed each factor, (including VI), within the metrics in order to assess the models' performance with respct to MICV. Based on this assessment it was expected that models showing a smaller VI, a larger PCC and a smaller RMSE would justify being labelled as performing well.

In analyzing the models' performance of the VI and PCC for MIDV, we found that for maximum temperature in both January and July, ACCESS1-0, GFDL-ESM2G, HadGEM2-ES and HadGEM2-CC showed a larger PCC and a smaller VI compared to the other models, suggesting that these models demonstrate a better ability to resolve the observed MIDV (Fig. 5(a)-(b)). Similarly, we also selected models showing a better ability for the other variables: ACCESS1-0, GFDL-ESM2G, HadGEM2-ES and HadGEM2-CC

for minimum temperature (Fig. 5(c)-(d)), ACCESS1-0, CanESM2, HadGEM2-ES and IPSL-CM5A-MR for wind speed (Fig. 5(e)-(f)) and ACCESS1-0, MIROC5, MIRCO-ESM-CHEM, and MPI-ESM-LR for precipitation (Fig. 5(g)-(h)), respectively.

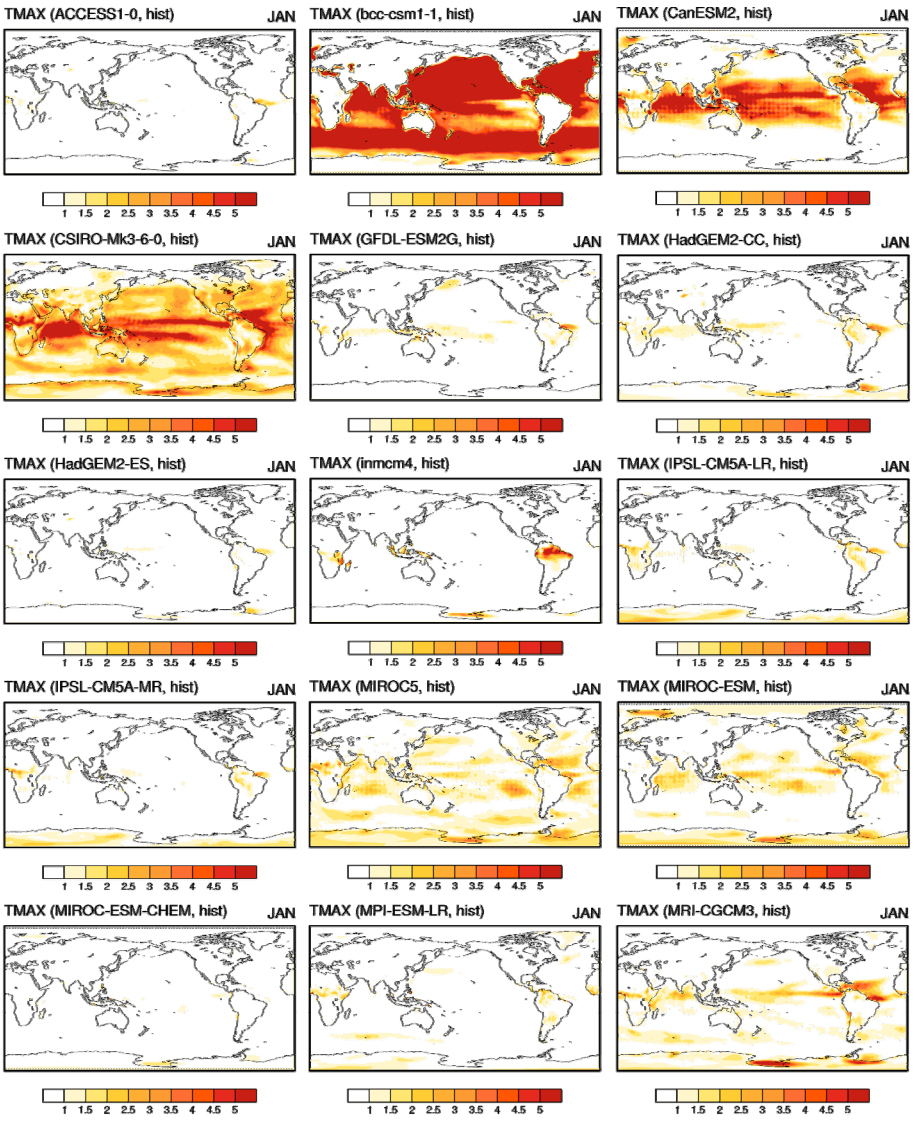

Figure 4 Variability Index (VI) for near surface maximum temperature in January calculated for 27 years from 1979 to 2005 using 15 CMIP5 models and reference datasets (reanalysis). Note that areas in dark red indicate a large departure from the reference datasets and vice-versa.

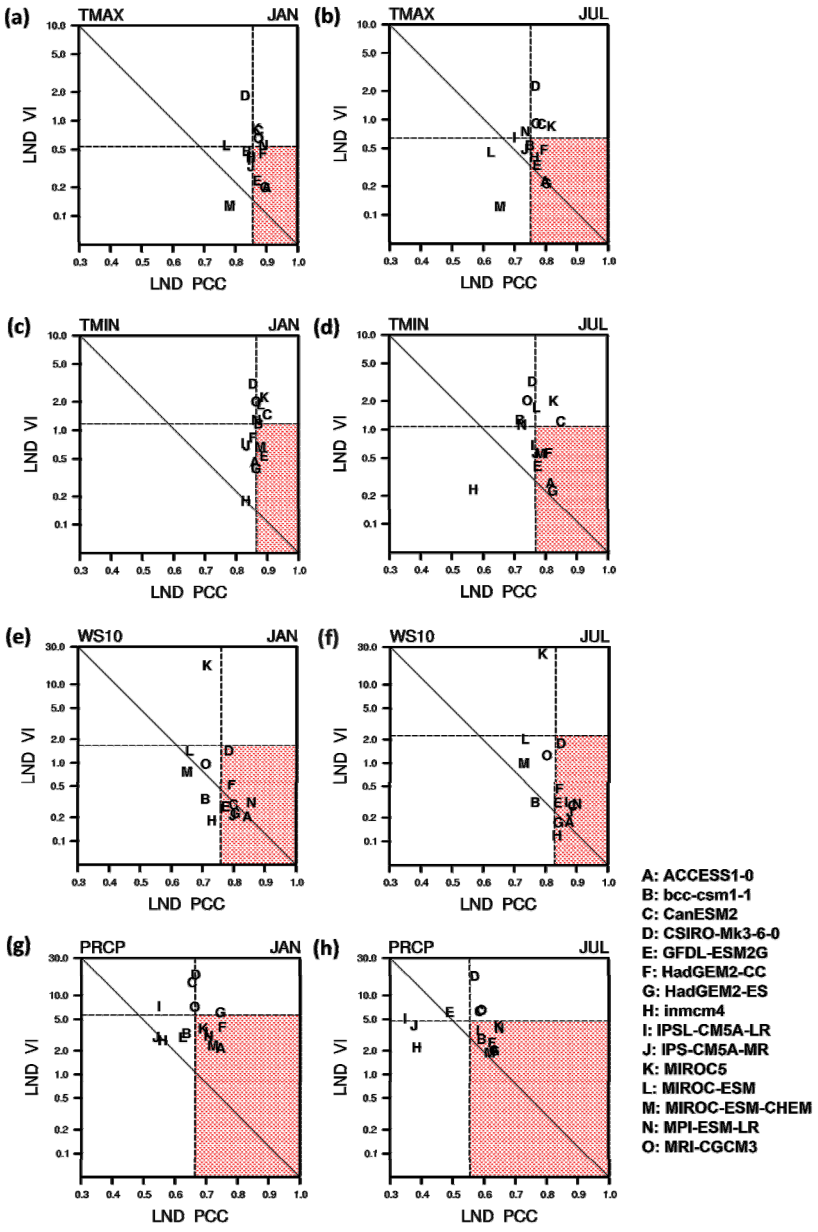

Figure 5 Scatter diagrams showing variability index (VI) versus pattern correlation coefficient (PCC) from each CMIP5 model averaged over land only: (a)-(b) near surface maximum temperature, (c)-(d) near surface minimum temperature and (e)-(f) near surface wind speed ranging from 1979 to 2005 (27 years) and (g)-(h) precipitation extending from 1997 to 2005 (9 years). Dashed lines indicate the median value of a models' VI or PCC, and solid lines are diagonals. Note that the scale is logarithmic on the y-axis.

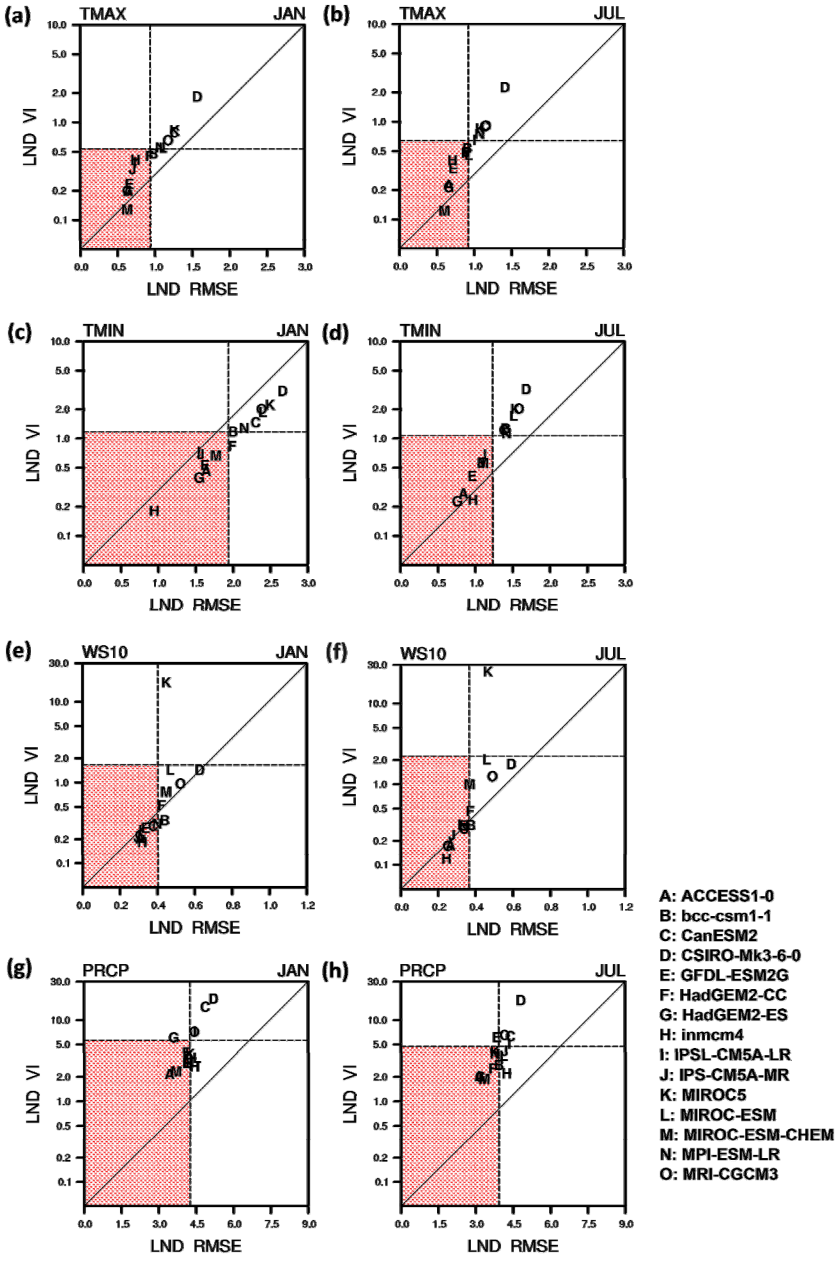

Figure 6 Scatter diagrams showing variability index (VI) versus root mean square error (RMSE) from each CMIP5 model averaged over land only: (a)-(b) near surface maximum temperature, (c)-(d) near surface minimum temperature and (e)-(f) near surface wind speed ranging from 1979 to 2005 (27 years) and (g)-(h) precipitation extending from 1997 to 2005 (9 years). Dashed lines indicate the median value of models' VI or PCC, and solid lines are diagonals. Note that the scale is logarithmic on the y-axis.

In addition, we evaluated the models' performance of VI and RMSE for MIDV. In examining those factors in the metrics, we found that for maximum temperature, ACCESS1-0, GFDL-ESM2G, HadGEM2-ES, and MIROC-ESM-CHEM showed a smaller RMSE and VI compared to the other models; indicating that these models exhibit a better ability of capturing the observed MIDV (Fig. 6(a)-(b)). We also determined which models showed a good ability to represent the observed MIDV for other variables: ACCESS1-0, GFDL-ESM2G, HadGEM2-ES and inmcm4 for minimum temperature (Fig. 6(c)-(d)), ACCESS1-0, HadGEM2-ES, inmcm4, and IPSL-CM5A-MR for wind speed (Fig. 6(e)-(f)) and ACCESS1-0, MIROC5, MIROC-ESM-CHEM, and MPI-ESM-LR for precipitation (Fig. 6(g)-(h)).

From the metrics (as shown in Fig. 5 and Fig. 6), we selected the top three models which showed the best ability to resolve observed MIDV for each variable: ACCESS1-0, GFDL-ESM2G, and HadGEM2-ES for maximum and minimum temperature, ACCESS1-0, HadGEM2-ES, and IPSL-CM5A-MR for wind speed and ACCESS1-0, MIROC5, and MPI-ESM-LR for precipitation. It is noteworthy that different models were chosen for different variables; however, ACCESS1-0 was commonly selected as the best model for all variables.

A comparison of simulated MIDV calculated from all 15 models (MMM15) with that from top three best models (BEST3) revealed that BEST3 were in high and good agreement with observed MIDV (Fig. 1(a)) for maximum temperature in January (Fig. 7(a)-(b)). MMM15 showed less variability of maximum temperature in the continents of the Northern Hemisphere high latitudes in January (Fig. 7(a)), whereas BEST3 exhibited a stronger variability in the same area which was close to that of the observation (Fig. 7(b)). For minimum temperature, BEST3 and MMM15 showed less variability in the extratropical continents in January (Fig. 7(c)-(d)) compared with that of the observed variability (Fig. 1(c)). However, the variability of BEST3 was relatively large compared with that of MMM15. In addition, MMM15 showed less variability of wind speed in the North Pacific and North Atlantic Ocean in January (Fig. 7(e)), while BEST3 represented a larger variability of wind speed in that area (Fig. 7(f)). Again, the variability of BEST3 agreed fairly well with that of the observed MIDV (Fig. 1(e)). Unlike other variables, simulated MIDV for precipitation exhibited

much less variability compared with that of observed MIDV(Fig. 1(g)), regardless of whether the MIDV was calculated from MMM15 or BEST3 (Fig. 7(g) and (h)). This was because of the difficulties inherent in the ability of climate models to resolve the spatio-temporal variability of precipitation (e.g., Cook and Vizy 2006; Johns *et al*. 2006; Lambert and Boer 2001). Nonetheless, BEST3 displayed a slightly higher variability than MMM15, especially over the western Atlantic Ocean, central parts of South America and some parts of Southeast Asia.

In January, BEST3 showed a more similar variability to the observed MIDV than did MMM15 for July (Fig. 8). For maximum temperature, BEST3 exhibited a higher variability than did MMM15 in the continents of the Southern Hemisphere high latitudes (Fig. 8(a) and (b)), which was closer to the observed MIDV. For minimum temperature, BEST3 showed a higher variability than did MMM15, but still less than the observed MIDV(Fig. 8(c) and (d)). A comparison of the variability for wind speed between MMM15 and BEST3 revealed that BEST3 showed a more similar variability to the observed MIDV(Fig. 8(e) and (f)). Simulated MIDV for precipitation from both MMM15 and BEST3 showed less variability than did the observed MIDV (Fig. 8(g) and (h)); however, BEST3 demonstrated slightly higher variability than that of MMM15 in some parts of the eastern Pacific Ocean, western Tropical Atlantic and some parts of Southeast Asia.

To conclude, using the metrics (including VI, PCC, and RMSE), we assessed the models' performance in resolving observed MIDV for each variable. In general, the simulated MIDV calculated from the top three best models (BEST3) showed a better performance compared to that of all the 15 models' means (MMM15). This indicates that (1) the metrics used in this study can be useful in assessing the models' performance; (2) based on the metrics, we can reasonably select the best models for resolving observed MIDV; and thus (3) we can expect that the best models selected can be used to project changes in simulated MIDV in a future climate.

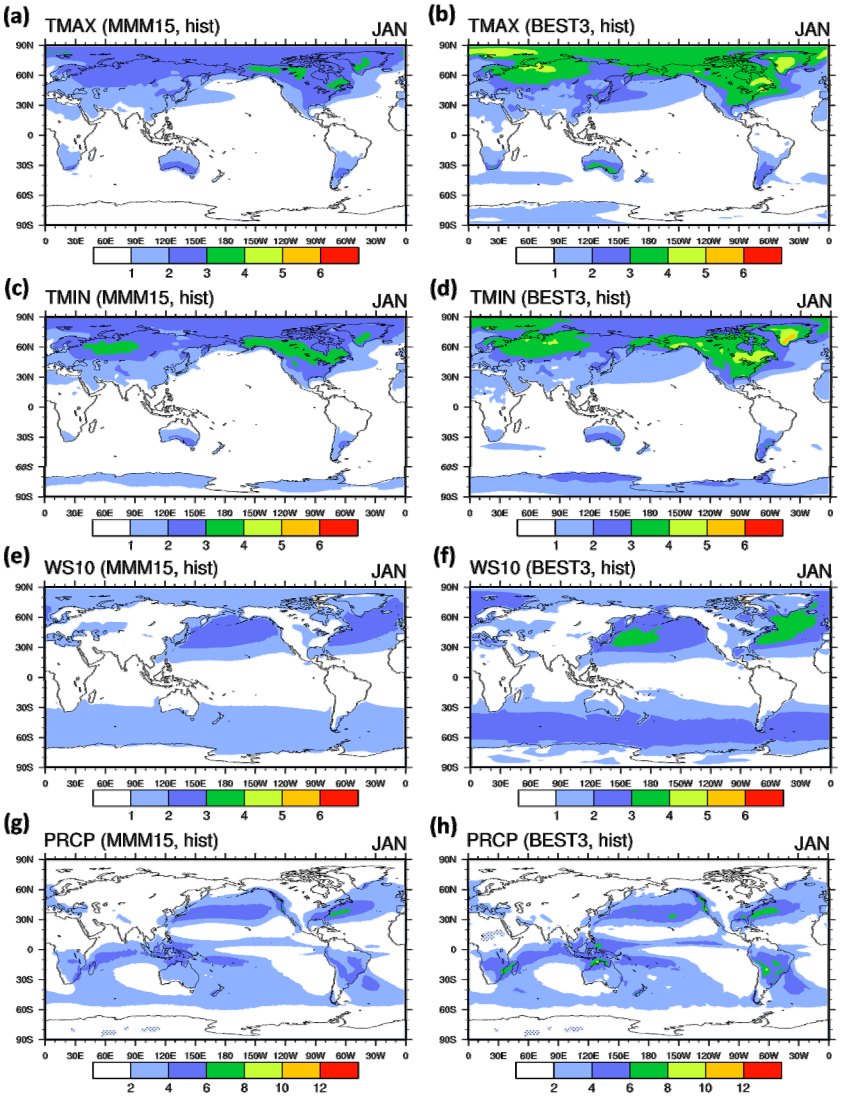

Figure 7 Simulated mean interdiurnal variability (MIDV) in each reanalysis dataset and observation: (a)-(b) 2-m maximum temperature, (c)-(d) 2-m minimum temperature, (e)-(f) 10-m wind speed in January for 27 years from 1979 to 2005 and (g)-(h) precipitation in January for nine years from 1997 to 2005. Left panel is for MIDV estimated from all 15 CMIP5 models (MMM15) and right panel is for MIDV from the top three best models (BEST3).

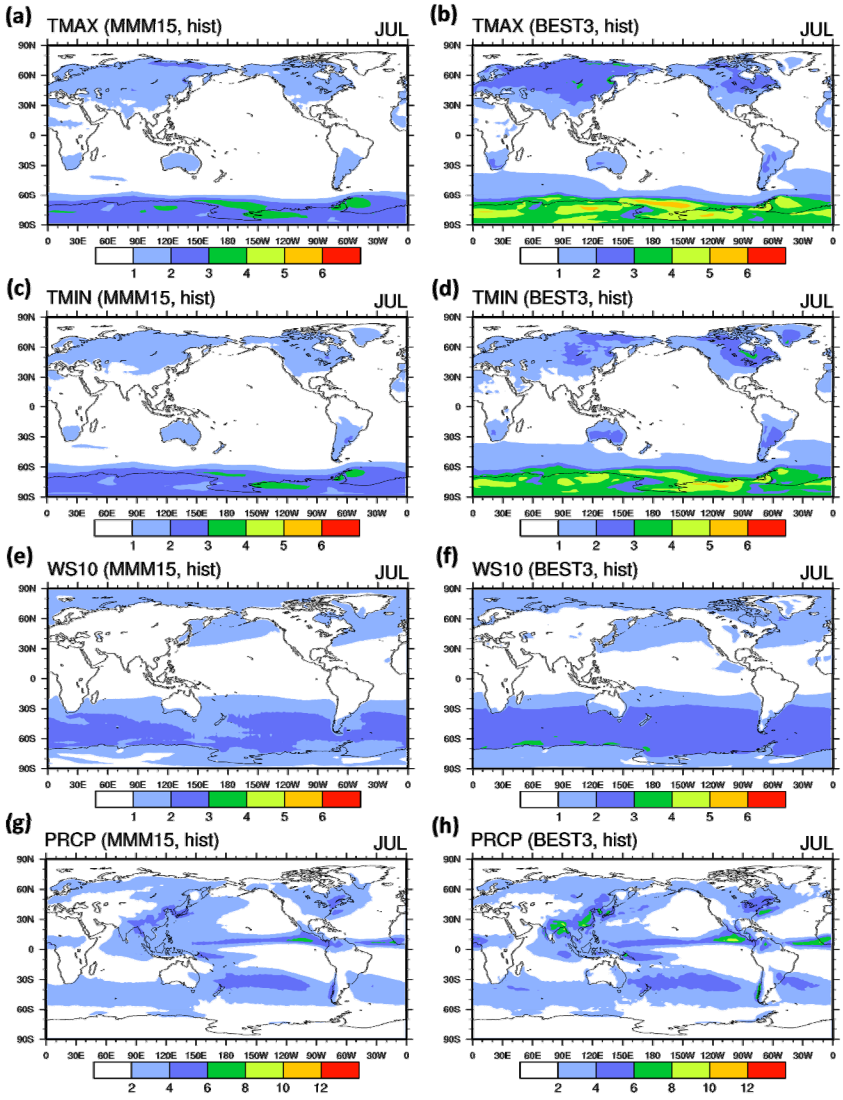

Figure 8 Simulated mean interdiurnal variability (MIDV) in each reanalysis dataset and observation: (a)-(b) 2-m maximum temperature, (c)-(d) 2-m minimum temperature, (e)-(f) 10-m wind speed in July for 27 years from 1979 to 2005 and (g)-(h) precipitation in January for nine years from 1997 to 2005. Left panel is for MIDV estimated from all 15 CMIP5 models (MMM15) and right panel is for MIDV from the top three best models (BEST3).

3.3 Simulated MIDV: Future projection

3.3.1 Near surface maximum and minimum temperature

Using the top three best models chosen for each variable, we calculated the signal-to-noise ratio of simulated MIDV for near surface maximum and minimum temperature in a future climate. It is important to consider projections for maximum and minimum temperature separately when assessing the impact of climate change, because the impact on certain societies and ecosystems will be directly related to changes in daily minimum or maximum temperature rather than to changes in daily mean temperature (Lobell *et al.* 2007).

In a future climate, in the middle to high latitudes of the Northern Hemisphere in January, (for example over North America and the northwestern part of Eurasia (Figs. 9(a)-(b) and Figs. 10(a)-(b)), there is a signal of noticeable reduction in the MIDV for surface maximum and minimum temperature. The magnitude of the reduction in the MIDV for maximum temperature is quite similar to that of minimum temperature over these regions; indicating that the day-to-day temperature variability is projected to decrease at a similar rate during both the day and night in January over those areas. However, under warmer climate conditions, forced by a doubling of CO_2, the reduction of the meridional gradient of temperature in the winter high latitudes leads to a reduction in the frequency or intensity of baroclinic disturbances, and thus a reduction in the day-to-day variability of near-surface temperature in the winter high latitudes where sea ice is replaced by open water (Cao *et al.* 1992). Unlike regions such as North America and the northwestern part of Eurasia, a general disparity between the maximum and minimum temperature uncertainty is observed in January. For example, there is a generally increased signal in the MIDV of maximum temperature over the northern part of South America and the southern part of Africa, whereas there is almost no change but noise in the MIDV of minimum temperature over these regions.

There is a signal of reduction in the MIDV for both maximum and minimum temperature in the high latitudes in April. However, the extent of the reduction of

the signal covers broader areas for minimum temperature than for maximum temperature (Figs. 9(c)-(d) and Figs. 10(c)-(d)). For maximum temperature, there is a signal of increase in the MIDV over regions such as the western part of North America and the northern part of South America, whereas for minimum temperature there is no clear change but the existence of noise in the MIDV over those regions.

Spatial patterns of changes in MIDV for maximum and minimum temperature in July (a warmer month) are different from those in other months (Figs. 9(e)-(f) and Figs. 10(e)-(f)). There is no clear signal of change in MIDV in the middle to high latitudes in July. The models project large increases in MIDV for maximum temperature over Europe, Africa, the eastern parts of Australia and the central and eastern parts of North America. The models also show little decrease in MIDV for minimum temperature over Africa, the eastern parts of Eurasia, the western parts of Australia and the northern and central parts of South America. These result agrees in part with information from literature. In a future climate, the daily mean temperature variability is projected to increase over land in the Northern Hemisphere summer and in the tropics (Kitoh and Mukano 2009). However, the signal of changes over these regions in July is not as obvious as in other months.

In October, there is again a signal of significant reduction in MIDV for both maximum and minimum temperature in the high latitudes, and the models project a signal of increase in MIDV for maximum temperature over regions such as Europe and parts of Africa. As in other months, the models project little decrease but they do project noise in the MIDV for minimum temperature over most land parts except those of the Northern Hemisphere high latitudes (Figs. 9(g)-(h) and Figs. 10(g)-(h)).

In analyzing future projections of changes in simulated MIDV for both maximum and minimum surface temperature, we found that there is a signal of marked reduction in the day-to-day variability for maximum and minimum temperature over high latitudes in cool seasons. In particular, the spatial extent of reduction in MIDV covers broader areas in January than in any other month. The models also show that there is a larger increase in the MIDV for maximum temperature in many areas, but there is little decrease in the MIDV for minimum temperature in broad areas. Changes in advection, having a substantial influence on day-to-day temperature variability,

could be one of the possible reasons for the difference in changes in the MIDV among regions (Cao *et al*. 1992). We also found that changes in MIDV for minimum temperature exhibit noise in more regions than do those for maximum temperature; suggesting the models' higher uncertainty in the MIDV projection for minimum temperature than for maximum temperature.

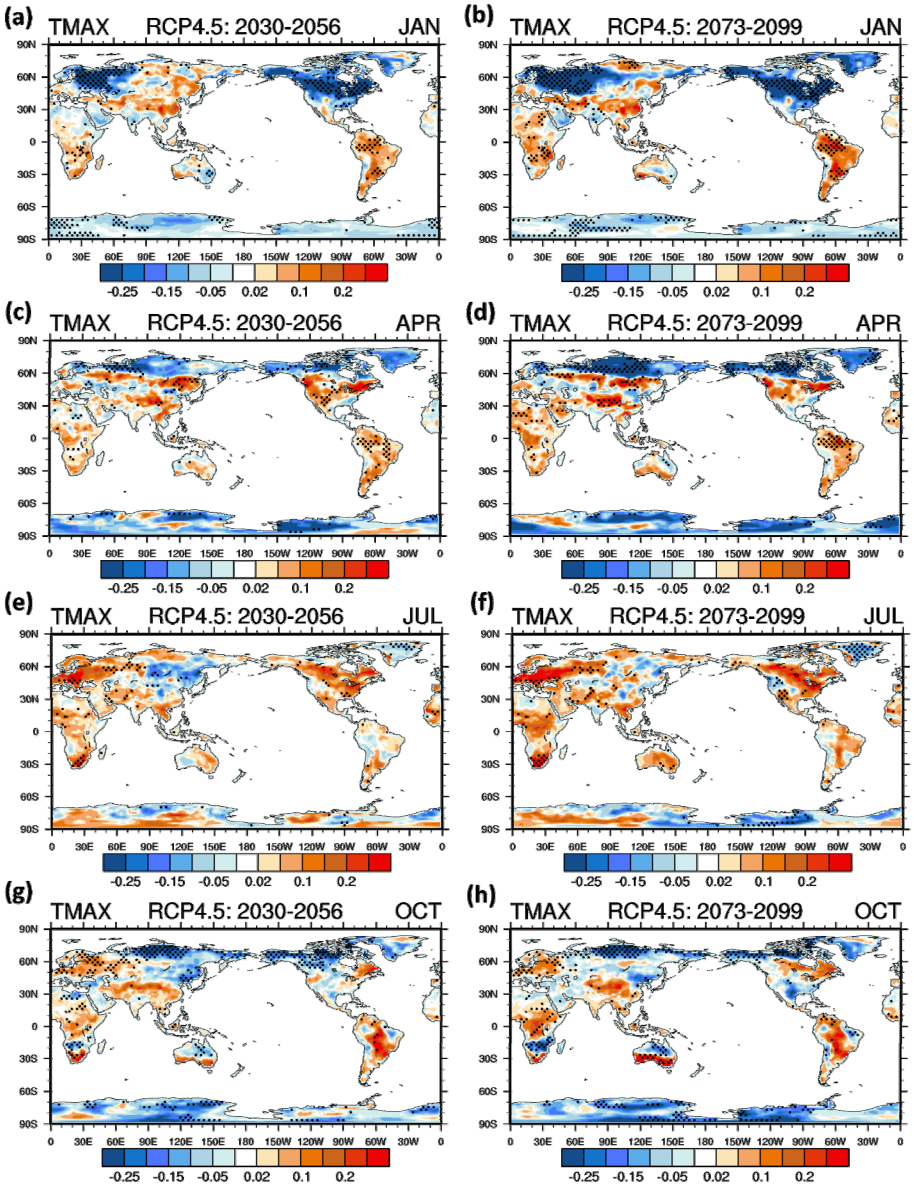

Figure 9 Future projected MIDV for near surface maximum temperature over land: in (a)-(b) January, (c)-(d) April, (e)-(f) July and (g)-(h) October. Left panel shows MIDV for the mid-21st century (2030–2056) and right panel for the late-21st century (2073–2099). Note that the shaded area indicates the multi-model's (top three best models) mean changes in MIDV. The stippling superimposed on the shaded areas shows that the magnitude of the multi-model's changes is greater than the inter-model standard deviation.

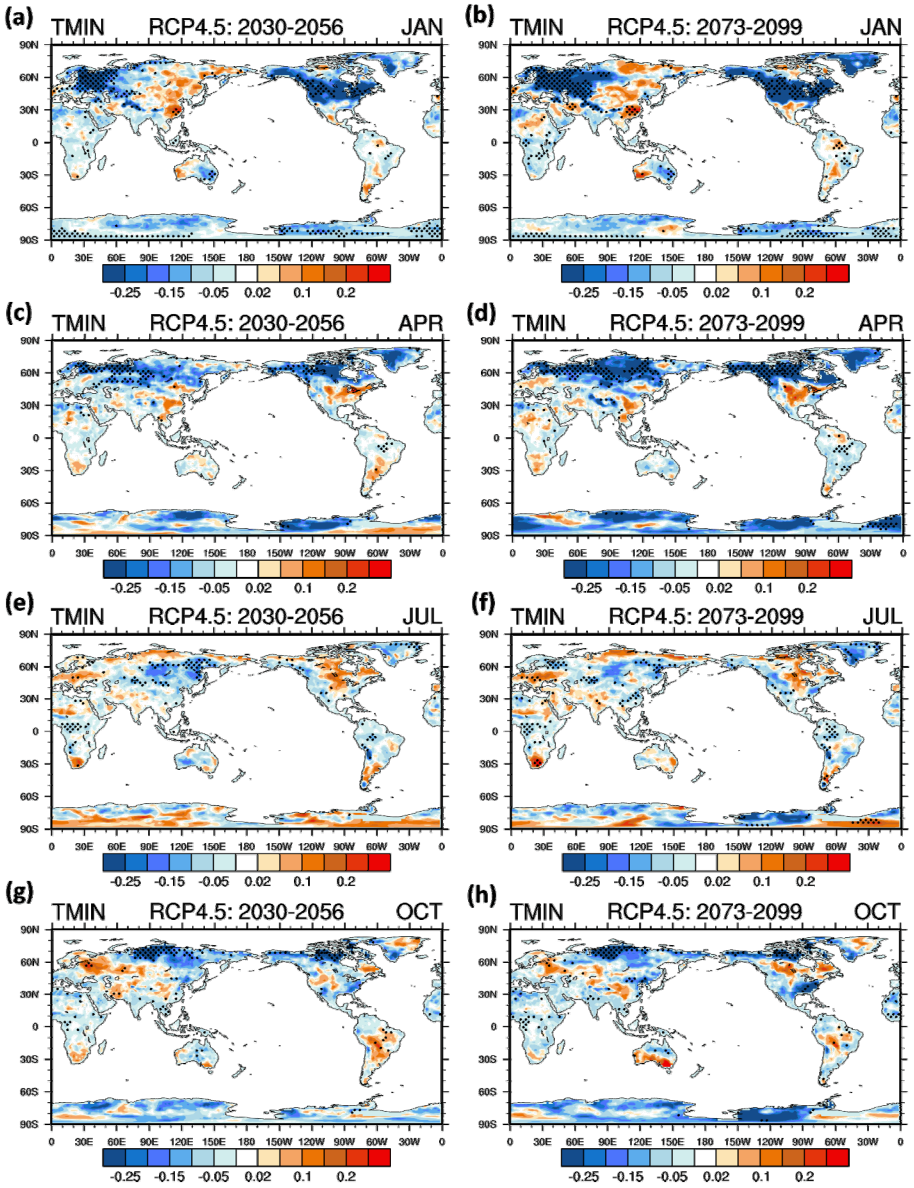

Figure 10 Future projected MIDV for near surface minimum temperature over land: in (a)-(b) January, (c)-(d) April, (e)-(f) July and (g)-(h) October. Left panel shows MIDV for the mid-21st century (2030–2056) and right panel for the late-21st century (2073–2099). Note that the shaded area indicates the multi-model's (top three best models) mean changes in MIDV. The stippling superimposed on the shaded areas shows that the magnitude of the multi-model's changes is greater than the inter-model standard deviation.

3.3.2 Near surface wind speed

The MIDV for wind speed exhibits a large uncertainty (noise) over many areas (Fig. 11) and there is no clear signal of change throughout most of the year. In January, there is a large increase in the MIDV over eastern parts of Eurasia, northern Africa and Europe, but a large reduction over North America, middle parts of the Eurasian continent and the southeastern parts of Australia (Figs. 11(a)-(b)). In the warmer months, such as April and July, there is a significant reduction in the MIDV over broader parts of the Eurasian continent and over North America (Figs. 11(c)-(f)). In particular, there is a significant reduction in the MIDV in July over the widest region of Eurasia and North America. In October, there is also a reduction in the MIDV over many parts of the Northern Hemisphere, but this represents noise and not signals.

In analyzing future projections of changes in simulated MIDV for surface wind speed, we found that there is a reduction in the day-to-day variability for surface wind speed over large parts of land in the Northern Hemisphere throughout most of the year, except for January. In particular, there is a signal of reduction in the MIDV over the continent of Eurasia and the western parts of North America in July. However, in other months there is almost no distinct signal over most land areas. Changes in MIDV for surface wind speed show more regional or local differences compared to those for surface maximum and minimum temperature. Spatial variations in changes in MIDV reflect differences in the frequency and intensity of periodic surface wind changes at the various locations.

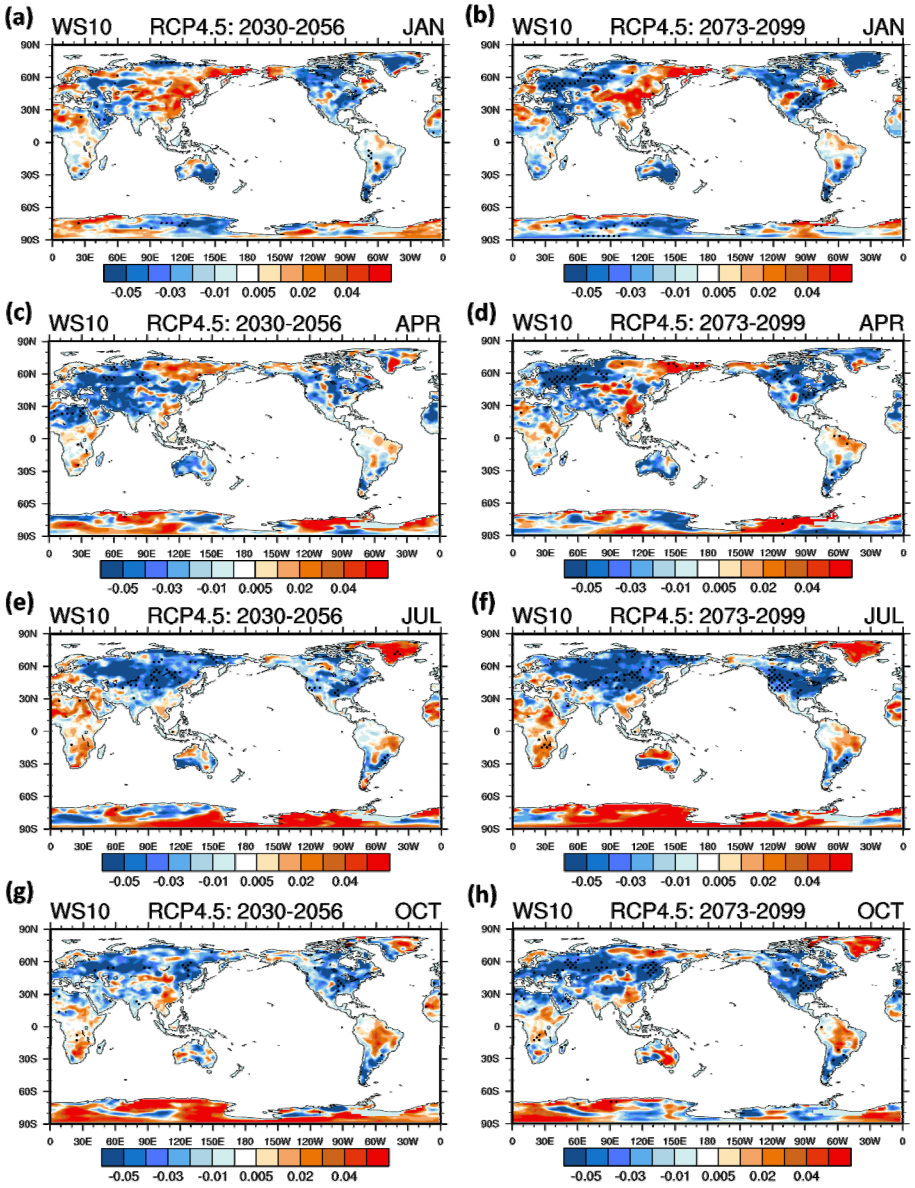

Figure 11 Future projected MIDV for near surface wind speed over land: in (a)-(b) January, (c)-(d) April, (e)-(f) July and (g)-(h) October. Left panel shows MIDV for the mid-21st century (2030-2056) and right panel for the late-21st century (2073-2099). Note that the shaded area indicates the multi-model's (top three best models) mean changes in MIDV. The stippling superimposed on the shaded areas shows that the magnitude of the multi-model's changes is greater than the inter-model standard deviation.

3.3.3 Precipitation

In a future climate, there is a signal of increase in the MIDV for precipitation in the middle to high latitudes in January. This means that the models show a similar tendency (less uncertainty) of increase in the MIDV for precipitation (Figs. 12(a)-(b)) over those regions. In addition, there is strong increase in the MIDV for precipitation over Southern Africa, Eastern Australia and the northern parts of South America, although there is a noise over those regions. In April, there is an increase in the MIDV for precipitation over broader regions, but most of them represent noise (large uncertainty). However, there is a signal of increase in the MIDV for precipitation over regions such as East Asia and Southeast Asia (Figs. 12(c)-(d)). In July, there is a signal of marked increase in the MIDV for precipitation over East Asia and Southeast Asia, but there is a noise of increase or decrease over other regions (Figs. 12(e)-(f)). In October, the spatial pattern is generally similar to that of April (Figs. 12(g)-(h)). There is a signal of increase in the MIDV for precipitation over East Asia and the eastern parts of North America. Unlike over land in the Northern Hemisphere, there is dipole-like pattern in changes in MIDV for precipitation over land in the Southern Hemisphere. For example, there is an increase in the MIDV for precipitation over middle parts of Africa (and central Australia, middle parts of South America), but there is a decrease over Southern Africa (and Eastern Australia, northeast parts of South America).

In analyzing future projections of changes in simulated MIDV for precipitation, we found that there is a noticeable signal of increase in the middle to high latitudes of the Northern Hemisphere in January. In particular, there is a signal of large increase over East Asia throughout most of the year, suggesting that the models show a similar tendency (less uncertainty) of an increase in the MDIV for precipitation over the region. In addition, the signal of changes in MIDV for precipitation is more obvious over land in the Northern Hemisphere than in the Southern Hemisphere.

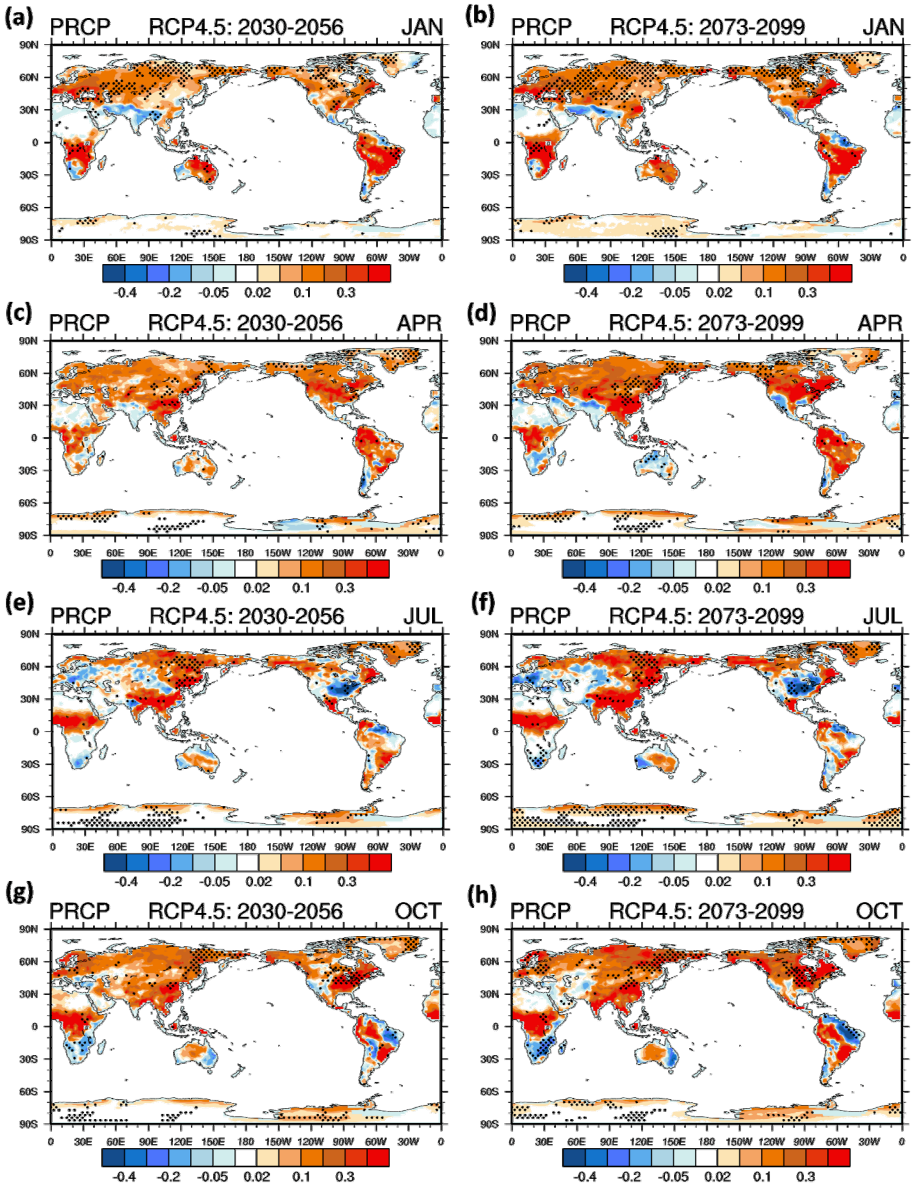

Figure 12 Future projected MIDV for precipitation over land: in (a)-(b) January, (c)-(d) April, (e)-(f) July and (g)-(h) October. Left panel shows MIDV for the mid-21st century (2030–2056) and right panel for the late-21st century (2073–2099). Note that the shaded area indicates the multi-model's (top three best models) mean changes in MIDV. The stippling superimposed on the shaded areas shows that the magnitude of the multi-model's changes is greater than the inter-model standard deviation.

4. SUMMARY AND CONCLUSION

Using a recently released, comprehensive global multi-model ensemble dataset formed by CMIP5 GCMs, we assessed the models' performance in terms of their ability to represent mean interdiurnal variability (MIDV) climatology for surface variables: surface maximum and minimum temperature and surface wind speed and precipitation, under present climatic conditions (i.e., 1997 to 2005 for precipitation and 1979 to 2005 for other variables). We found that some models revealed a similar magnitude and pattern between simulated and observed MIDV, and the remaining models showed a similar pattern but a weaker magnitude than the observed MIDV. This feature of simulated MIDV was shown for variables such as surface maximum and minimum temperature and surface wind speed throughout most of the year. However, the magnitude of simulated MIDV for precipitation was much weaker than that of the observed MIDV.

Using three different verification measures, including the pattern correlation coefficient (PCC), root-mean square error (RMSE) and variability index (VI), we also quantitatively evaluated the models' performance in their ability to represent the observed MIDV. The variability index is a newly proposed measure that can quantitatively reveal how well a model can resolve the observed MIDV. Based on statistics from these three verification measures, we selected the top three models for resolving the observed MIDV for each surface variable. As a result we chose different "best models" for different variables, regardless of months or seasons. The models selected as the "best models" are as follows: ACCESS1-0, GFDL-ESM2G, and HadGEM2-ES for maximum and minimum temperature, ACCESS1-0, HadGEM2-ES, and IPSL-CM5A-MR for wind speed and ACCESS1-0, MIROC5, and MPI-ESM-LR for precipitation. It is a noteworthy result that ACCESS1-0 was commonly selected as a "best model" across all variables.

Using an ensemble mean of MIDV from the top three models chosen separately for each surface variable, we also examined the signal-to-noise ratio of simulated MIDV in a future climate. In analyzing future projections for changes in simulated MIDV of maximum and minimum surface temperature, we found that the signal of

marked reduction in the MIDV was obvious over high latitudes, particularly in cool seasons. This reduction signal was much more noticeable in January than in any other month. The models also showed a larger increase in the MIDV for maximum temperature and a slight decrease for minimum temperature. In addition, we found that the models showed a higher uncertainty in the MIDV for the minimum temperature than for the maximum temperature.

We found that there was a reduction in the MIDV for surface wind speed over large land areas in the Northern Hemisphere throughout most of the year, except for in January. In particular, a relatively clear signal of reduction was evident over the continent of Eurasia and the western parts of North America in July. However, the models revealed large spatial variations of changes in MIDV for surface wind speed, compared with those for other surface variables. We also found that there was a signal of noticeable increase in the MIDV for precipitation in the middle to high latitudes of the Northern Hemisphere in January. In addition, there was a signal of large increase in the MIDV for precipitation over East Asia throughout most of the year.

This study suggests a possible change in the characteristics of weather (day-to-day) under future climate conditions. These changes in the features of future weather conditions should be considered as important as those of mean climate change, because the increasing risk of extremes is related to the variability on daily time scales as well as to mean climate change. For instance, most impacts of heat waves on societies and ecosystems act on daily and weekly time sales (e.g., Fischer and Schär 2009).

From this study, it is still unclear what kind of environmental conditions could lead to the changes in MIDV for each surface variable under future climate conditions. It is known that the MIDV may be related to mid-tropospheric circulation patterns (Williams and Parker, 1997) or synoptic disturbances (Kitoh and Mukano, 2009). Therefore, it is considered that future studies are needed to examine changes in the atmospheric circulation patterns and/or synoptic disturbances associated with changes in MIDV at the surface. That is, the inclusion of phenomena that leads to large-scale atmospheric circulation or oceanic conditions could further explain the changes in day-to-day variability in a future climate. Attributing land surface processes

to the MIDV variability on the surface would also be an important subject area for exploration in future studies.

Several other issues also remain to be solved through further in-depth studies. For example, the physical basis for the functional relationship between day-to-day variability and changes in extremes for a certain variable, are yet to be clarified. Various research has assessed the change in climate extremes (Easterling *et al.*, 2000; Frich *et al.*, 2002; Klein Tank and Können, 2003; Alexander *et al.*, 2006). However, few systematic and extensive studies have been conducted on the relationship between changes in extreme climatic events and day-to-day variability at the surface, even though future changes in daily variability at the surface are associated with extremes and will thus have a significant influence on our life and on several application sectors (Kitoh and Mukano 2009). Furthermore, the utilization of modeling data on a much finer spatial scale, through various dynamical and/or statistical techniques, would allow for the study of the relationship between regional or local factors and the day-to-day variability on the surface over specific areas.

REFERENCES

Alexander, L. V., Arblaster, J. M. (2009), Assessing trends in observed and modeled climate extremes over Australia in relation to future projections. Int J Climatol 29:417-435. doi: 10.1002/joc.1730

Alexander, L.V., Arblaster J.M. (2009) Assessing trends in observed and modeled climate extremes over Australia in relation to future projections. Int J Climatol 29:417-435. doi: 10.1002/joc.1730

Alexander, L.V., Zhang, X., Peterson, T.C., Caesar, J., Gleason, B., Klein Tank, A.M.G., Haylock, M., Collins, D., Trewin, B., Rahimzadeh, F., Tagipour, A., Rupa Kumar, K., Revadekar, J., Griffiths, G., Vincent, L., Stephenson, D.B., Burn, J., Aguilar, E., Brunet, M., Taylor, M., New, M., Zhai, P., Rusticussi, M., Vazquez-Aguirre, J.L. (2006) Global observed changes in daily climate extremes of temperature and precipitation. J Geophys Res 111, doi: 10.1029/2005JD006290.

Bolvin, D.T., Adler, R.F., Huffman, G.J., Nelkin, E.J., Poutiainen, J.P. (2009) Comparison of GPCP monthly and daily precipitation estimates with high-latitude gauge observations. J Appl Meteor Climatol 48:1843-1857

Cao, H.X., Mitchell, J.F.B., Lavery, J.R. (1992) Simulated diurnal range and variability of surface temperature in a global climate model for present and doubled CO2 climates. J Clim 5:920-943

Clarke, L.E., Edmonds, J.A., Jacoby, H.D., Pitcher, H., Reilly, J.M., Richels, R. (2007) Scenarios of greenhouse gas emissions and atmospheric concentrations. Sub-report 2.1a of Synthesis and Assessment Product 2.1. Climate Change Science Program and the Subcommittee on Global Change Research, Washington DC

Cook, K.H., Vizy, E.K. (2006) Coupled model simulations of the West African monsoon system: 20th century simulations and 21st century predictions J Clim 19:3681-3703

Dee, D.P., Uppala, S.M., Simmons, A.J., Berrisford, P., Poli, P., Kobayashi, S., Andrae, U., Balmaseda, M.A., Balsamo, G., Bauer, P., Bechtold, P., Beljaars, A.C.M., van de Berg, L., Bidlot, J., Bormann, N., Delsol, C., Dragani, R., Fuentes, M., Geer, A.J., Haimberger, L., Healy, S.B., Hersbach, H., Hólm, E.V., Isaksen, L., Kållberg, P., Köhler. M,, Matricardi, M., McNally, A.P., Monge-Sanz, B.M., Morcrette, J-J., Park, B.K., Peubey, C., de Rosnay, P., Tavolato, C., Thépaut, J-N., Vitart, F. (2011) The ERA-Interim reanalysis: configuration and performance of the data assimilation system. Q J R Meteorol Soc 137:553–597. doi: 10.1002/qj.828

Deser, C., Phillips, A., Bourdette, V., Teng, H. (2012) Uncertainty in climate change projections: the rule of internal variability. Clim Dyn 38:527-546. doi: 10.1007/s00382-010-0977-x

Driscol, D.M., Rice, P.B., Fong, J.M.Y. (1994) Spatial variation of climatic aspects of temperature: interdiurnal variability and lag. Int J Climatol 14:1001-1008. doi:10.1002/joc.3370140905

Easterling, D.R., Evans, J.L., Groisman, P.Y., Karl, T.R., Kenkel, K.E., Ambenje, P. (2000) Observed variability and trends in extreme climate events: a brief review. Bull AM Meteorol Soc 81:417-425

Fischer, E.M., Schär, C. (2009) Future changes in daily summer temperature variability: driving processes and role for temperature extremes. Clim Dyn 33:917-935

Frich, P.L., Alexander, V., Della-Marta, P., Gleason, B., Haylock, M., Klein Tank, A.M.G., Peterson, T. (2002) Observed coherent changes in climate extremes during the second half of the twentieth century Clim Res 19:193-212

Gebremichael, M., Krajewski, W.F., Morrissey, M.L., Huffman, G.J., Adler, R.F. (2005) A detailed evaluation of GPCP 1° Daily Rainfall Estimates over the Mississippi River Basin. J Appl Meteor 44:665-681

Gleckler, P.J., Taylor, K.E., Doutriaux, C. (2008) Performance metrics for climate models. J Geophys Res 113: D06104, doi:10.1029/2007JD008972

Hagemann, S., Jacob, C. (2007) Gradient in the climate change signal of European discharge predicted by a multi-model ensemble. Clim Change 81:309-327.

Hibbard, K.A., Meehl, G.A., Cox, P., Friedlingstein, P. (2007) A strategy for climate change stabilization experiments. EOS 99: 217, 219, 221

Huffman, G.J., Adler, R.F., Morrissey, M.M., Curtis, S., Joyce, R., McGavock, B., Susskind, J. (2001) Global precipitation at one-degree daily resolution from multi-satellite observations. J. Hydrometeor 2:36-50

IPCC (2007) Climate Change 2007: The Physical Science Basis. Contribution of Working Group I to the Fourth Assessment Report of the IPCC [Solomon, S., D. Qin, M. Manning, Z. Chen, M. Marquis, K. B. Averyt, M. Tignor and H. L. Miller (eds.)]. Cambridge University Press, Cambridge, United Kingdom and New York, NY, USA

Johns, T.C., Durman, C.F., Banks, H.T., Robert, M.J., McLaren, A.J., Ridley, J.K., Senior, C.A., Williams, K.D., Jons, A., Richard, G.J., Cusack, S., Ingram, W.J., Crucifix, M., Sexton, D.M.H., Joshi, M.M., Dong, B.W., Spencer, H., Hill, R.S.R., Gregory, J.M., Keen, A.B., Pardaens, A.K., Lowe, J.A., Bodas-Salcedo, A., Stark, S., Searl, Y. (2006) The New Hadley Center Climate Mode l(HadGEM1): Evaluation of coupled simulations. J Clim 19:1327-1353

Kanamitsu, M., Ebisuzaki, W., Woolen, J., Yang, S.K., Hnilo, J.J., Fiorino, M., Potter, G.L. (2002) NCEP–DOE AMIP-II Reanalysis (R-2). Bull Amer Meteor Soc 83:1631-1643

Kitoh, A., Mukano, T. (2009) Changes in daily and monthly surface air temperature variability by multi-model global warming experiments. J Meteor Soc Japan 87:513-524

Klein Tank, A.M.G., Können, G.P. (2003) Trends in indices of daily temperature and precipitation extremes in Europe, 1946-99. J Clim 16:3665-3680

Lambert, S.J., Boer, G.J. (2001) CMIP1 evaluation and intercomparison of coupled climate models Clim Dyn 17:83-106

Lobell, D.B., Bonfils, C., Duffy, P.B. (2007) Climate change uncertainty for daily minimum and maximum temperatures: A model inter-comparison. Geophys Res Lett 34, L05715, doi:10.1029/2006GL028726

Meehl, G.A., Hibbard, K.A. (2007) A strategy for climate change stabilization experiments with AOGCMs and ESMs. WCRP Informal Report No. 3/2007, ICPO Publication No. 112, IGBP Report No. 57, World Climate Research Programme: Geneva, 35 pp

Pincus, R., Batstone, C.P., Hofmann, J.P., Taylor, K.E., Glecker, P.J. (2008) Evaluating the present-day simulation of clouds, precipitation, and radiation in climate models J Geophys Res 113, D14209, doi:10.1029/2007JD009334

Prudhomme, C., Reynard, N., Crooks, S. (2002) Downscaling of global climate models for flood frequency analysis: where are we now? Hydrol Process 16:1137-1150

Rienecker, M.M., Suarez, M.J., Gelaro, R., Todling, R., Bacmeister, J., Liu, E., Bosilovich, M.G., Schubert,

S.D., Takacs, L., Kim, G.K., Bloom, S., Chen, J., Collins, D., Conaty, A., da Silva, A., Gu, W., Joiner, J., Koster, R.D., Lucchesi, R., Molod, A., Owens, T., Pawson, S., Pegion, P., Redder, C.R., Reichle, R., Robertson, F.R., Ruddick, A.G., Sienkiewicz, M., Woollen, J. (2011) MERRA: NASA's Modern-Era Retrospective Analysis for Research and Applications. J. Clim 24:3624-3648

Rosenthal S.L. (1960) The interdiurnal variability of surface-air temperature over the north Atlantic ocean. J Meteor 17:1-7

Saha, S., Moorthi, S., Pan, H-L., Wu, X., Wang, J., Nadiga, S., Tripp, P., Kistler, R., Woollen, J., Behringer, D., Liu, H., Stokes, D., Grumbine, R., Gayno, G., Wang, J., Hou, Y-T., Chuang, H-Y., Juang, H.M.H., Sela, J., Iredell, M., Treadon, R., Kleist, D., Delst, P.V., Keyser, D., Derber, J., Ek, M., Meng, J., Wei, H., Yang, R., Lord, S., Dool, H.V.D., Kumar, A., Wang, W., Long, C., Chelliah, M., Xue, Y., Huang, B., Schemm, J.K., Ebisuzaki, W., Lin, R., Xie, P., Chen, M., Zhou, S., Higgins, W., Zou, C.Z., Liu, Q., Chen, Y., Han, Y., Cucurull, L., Reynolds, R.W., Rutledge, G., Goldberg, M. (2010) The NCEP Climate Forecast System reanalysis. Bull Amer Meteor Soc 91:1015-1057

Santer, B.D., Mears, C., Doutriaux, C., Caldwell, P., Gleckler, P.J., Wigley, T.M.L., Solomon, S., Gillett, N.P., Ivanova, D., Karl, T.R., Lanzante, J.R., Meehl, G.A., Stott, P.A., Taylor, K.E., Thorne, P.W., Wehner, M.F., Wentz, F.J. (2011) Separating signal and noise in atmospheric temperature changes: the importance of timescale J Geophys Res 116, D22105, doi:10.1029/2011JD016263

Scherrer, S.C. (2011) Present-day interannual variability of surface climate in CMIP3 models and its relation to future warming. Int J Climatol 31:1518-1529. doi: 10.1002/joc.2170

Smith, S.J., Wigley, T.M.L. (2006) MultiGas forcing stabilization with minicam. The Energy Journal Special issue #3:373–392

Sushama, L., Laprise, R., Caya, D., Frigon, A., Slivitzky, M. (2006) Canadian RCM projected climate-change signal and its sensitivity to model errors. Int J Climatol 26:2141-2159.

Szczypta, C., Calvet, J-C., Albergel, C., Balsamo, G., Boussetta, S., Carrer, D., Lafont, S., Meurey, C. (2011) Verification of the new ECMWF ERA-Interim reanalysis over France. Hydrol Earth Syst Sci 15:647-666. doi:10.5194/hess-15-647-2011

Taylor, K.E. (2001) Summarizing multiple aspects of model performance in a single diagram. J Geophys Res 106:7183-7192

Taylor, K.E., Stouffer, R.J., Meehl, G.A. (2012) An overview of CMIP5 and the experiment design. Bull Amer Meteor Soc 93:4850498. doi:10.1175/BAMS-D-11-00094.1

Williams, K.R.S., Parker, K.C. (1997) Trends in interdiurnal temperature variation for the central United States, 1945-1985. The professional geographer 49:342-355. doi: 10.1111/0033-0124.00082

Wise, M., Calvin, K., Thomson, A., Clarke, L., Bond-Lamberty, B., Sands, R., Smith, S.J., Janetos, A., Edmonds, J. (2009) Implications of limiting CO2 concentrations for land use and energy. Science 324:1183–1186

Yin, X., Gruber, A., Arkinc, P. (2004) Comparison of the GPCP and CMAP Merged Gauge-Satellite Monthly Precipitation Products for the Period 1979-2001. J Hydromet 5:1207-1222

APCC TECHNICAL REPORT 2012-03

- An Assessment of Reliability in Climate Projections : Cloud Variation
- An Evaluation of the Ability of CMIP5 Multi-Models to Predict Interdiurnal Variability
- Climate Change Projection of South Asian Summer Monsoon
- The Role of the Western Pacific Oscillation Teleconnection Pattern

APEC Climate Center

12, Centum 7-ro, Haeundae-gu, Busan 612-020,
Republic of Korea
Tel: +82-51-745-3900 Fax: +82-51-745-3949
www.apcc21.org

비매품
9 788997 133387
ISBN 978-89-97333-38-7
ISBN 978-89-97333-35-6 (세트)